# Control of Single-phase Double Boost Effect AC-DC Converter

**A. Dieng, J.C. Le Claire, M.F. Benkhoris and M. Ait-Ahmed**
Institut de Recherche en Energie Electrique de Nantes Atlantique 37 Bd de l'université
BP406, 44602 Saint-Nazaire, France Tel.: +33 / (0) – 2.40.17.26.91 Fax: +33 / (0) – 2.40.17.26.18.
Mail: abdoulaye.dieng@univ-nantes.fr

***Abstract:*** *This paper investigates the Control Strategy of the Single-phase Unidirectional Double Boost Effect Rectifier. A double closed control loops strategy with a current inner loop and a voltage extern loop is investigated. In order to improve the performances of the single-phase unidirectional VIENNA rectifier, a coil is added in the structure of the converter. The new structure is called "DBE". These structures operate in continuous current and PFC modes thanks to an AC side current control. An optimal current control strategy is developed based on the use of an analog current controller. This one operates in sliding mode with a control of the maximum switching frequency of the power switches. Experimental results show the accurate tracking of the proposed analog current controller and confirm the advantages of the DBE compared to the single-phase VIENNA. Finally, a DC voltage controller is synthetized based on the power conservation and implemented in a Dspace system. Experimental results highlight the DC voltage control loop.*

***Key words:*** *Double Boost Effect Rectifier, Converter control, DC Voltage Control*

## 1. Introduction

Many applications using AC/DC power electronics converters require more reliability and high quality power sources. In the literature many rectifiers topologies are investigated [1, 2, 4-9]. In [4] a review of single-phase improved power quality AC-DC converter is done. More than 450 research publications are given. The current from the AC source of the classical converter using diode rectifiers or thyristor rectifiers is not non-sinusoidal and its harmonic distorsion is very high. One of the solutions to eliminate the current harmonics and to compensate the reactive power is the power factor correctors techniques. Thereby, in this paper, a new rectifier is presented. It is named the Double Boost Effect "DBE" rectifier [2]. Its core involves a single switch, six diodes and two coils. Nevertheless, when the coil L2 (see Fig.1) value is equal to zero, it is similar to the single-phase VIENNA power cell [3]. Moreover, many research works have focused on DC bus voltage control of rectifiers AC/DC [6-8] [10-12]. In [6] the authors investigate the voltage control of a three-phase unity power factor AC/DC converter with midpoint connection and they propose the control of the two intermediate capacitor voltages. Also in [10] three solutions for the DC voltage control are proposed. For each solution the experimental results show the performances of these control systems. For all these works, this is the value of the DC bus voltage which is controlled. One of the drawbacks is that the parameters of the voltage regulator can depend on the operating point and load parameters. This is a drawback when the load is non-linear. To solve this problem, the load is considered as a disturbance, and the square of the DC voltage value is now uses for a better control.

Even if the DBE rectifier has been investigated in [2], nevertheless the current control was done on the coil L2 (see Fig.1). Here, the DBE current control is done on the coil L1 (see Fig.1) and this improves the AC side current THD. So, the next figure (Fig.1) illustrates the whole system.

The whole control is composed by an inner current loop and an extern voltage one. The current controller is an analog circuit which operates in sliding mode and controls the maximum switching frequency of the single switch. It also permits to have a low input current distortion and a high PFC and it has already been used in AC/DC conversion [8]. For the external voltage control loop, a digital controller is used and it is implemented in a Dspace system.

At the beginning, a study of the DBE rectifier is done focusing on the current control performances and then a comparison with the power cell of the single-phase VIENNA rectifier is done too. So the AC current controller is presented. Thereafter, the DC voltage is introduced. Experimental results highlight the control strategy proposed.

## 2. Single-phase unidirectional AC/DC converter

Fig. 2 presents the general structure of the so called DBE single phase AC/DC converter, where the known VIENNA structure can be easily deduced by imposing the value of the coil $L_2$ equals to zero.

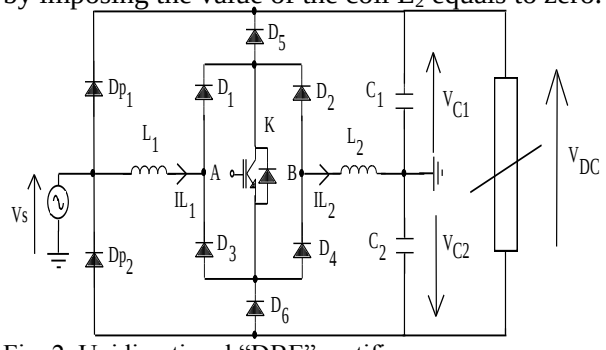


Fig. 2. Unidirectional "DBE" rectifier

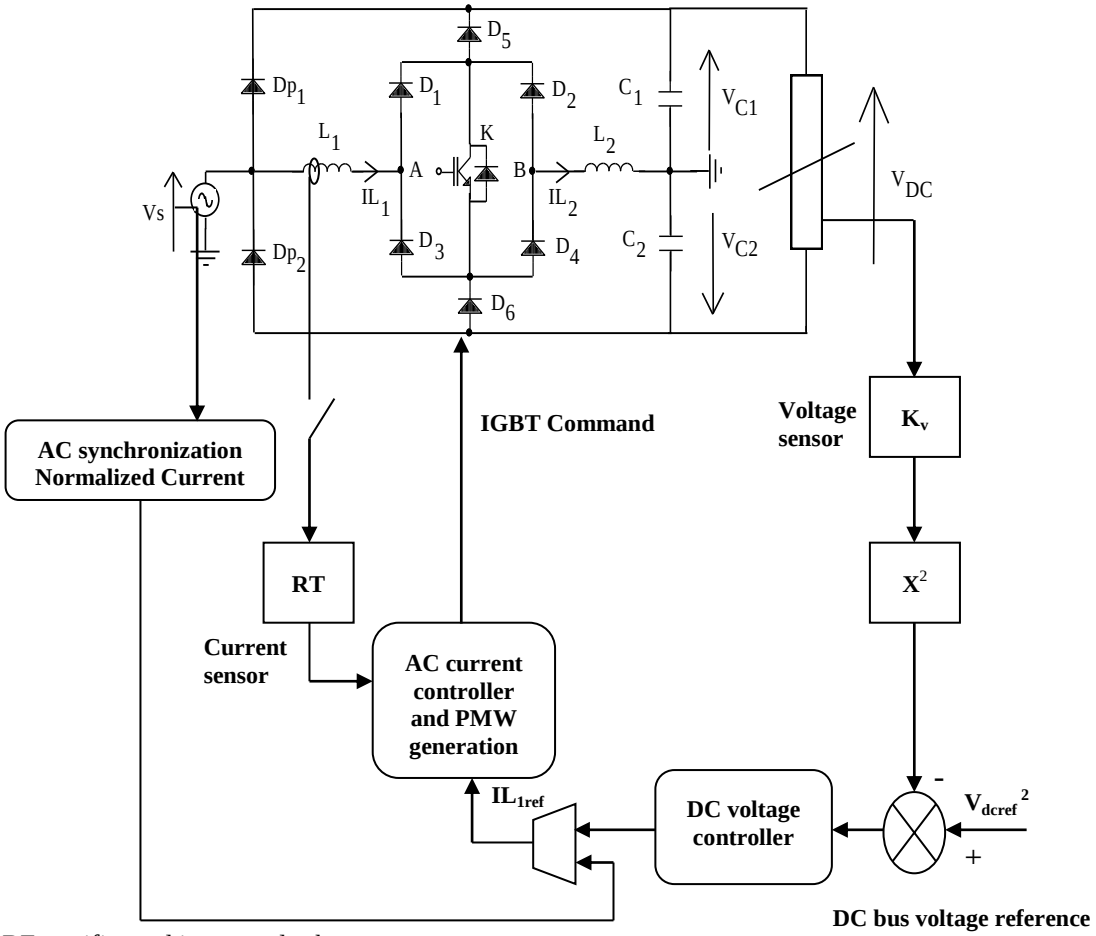


Fig. 1: DBE rectifier and its control scheme

Now, the study starts with DBE rectifier states where the semi-conductors are considered ideals and the rectifier is unloaded. The diodes Dp1 and Dp2 (see Fig. 2) are used to respectively preload the capacitors $C_1$ and $C_2$ during the first positive and negative half-periods of the mains voltage (Vs). Then the rectifier operates in continuous and PFC modes as the power on transient is finished.

### 2.1 Positive mains voltage

When the switch K is closed (see Fig. 3 (a)), the diodes D1 and D4 are in the ON states and the current goes through the coil $L_1$, the diode D1, the switch K, the diode D4 and the coil $L_2$. Therefore the coils $L_1$ and $L_2$ store energy.

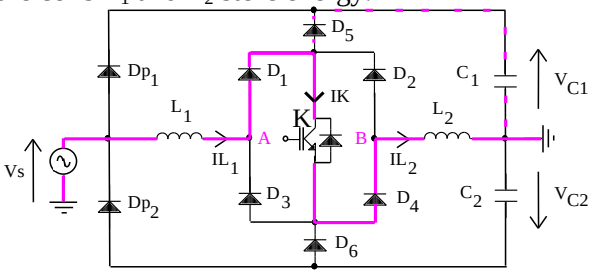


(a)

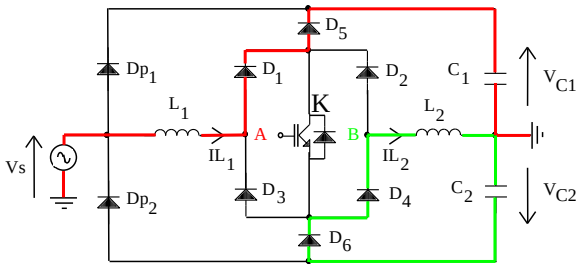


(b)

Fig. 3. Positive current paths: (a) closed switch, (b) open switch [3]

During a very short time, a small part of the current $i_{L1}(t)$ goes to the diode D5 and the capacitor $C_1$. The next equations result [3]:

$$Vs(t) - L_1 \frac{d}{dt} i_{L1}(t) = L_2 \frac{d}{dt} i_{L2}(t) \quad (1)$$

$$i_{L2}(t) = i_K(t) = i_{D4}(t) \quad (2)$$

$$i_{L1}(t) = i_{D1}(t) = i_{D5}(t) + i_K(t) \quad (3)$$

$$i_{D5}(t) > 0 \quad (4)$$

$$i_{L1}(t) > i_{L2}(t) \quad (5)$$

$$i_{D5}(t) = i_{L1}(t) - i_{L2}(t) \quad (6)$$

$$V_{D5}(t)=0 \quad (7)$$

After the short time the diode D5 turns off and the currents $i_{L1}(t)$ and $i_{L2}(t)$ are equals [3]:

$$i_{D5}(t)=0 \quad (8)$$

$$V_{D5}(t)=Vs(t)-L_1\frac{d}{dt}i_{L1}(t)-V_{C1}(t) \quad (9)$$

Furthermore the following equations are always verified [3]:

$$i_{D2}(t)=i_{D3}(t)=i_{D6}(t)=0 \quad (10)$$

$$V_{D1}(t)=V_{D4}(t)=0 \quad (11)$$

$$V_{D6}(t)=V_{C2}(t)-Vs(t)+L_1\frac{d}{dt}i_{L1}(t) \quad (12)$$

When the switch K is open (see Fig. 3 (b)), the diodes D1, D5, D6 and D4 are in the ON states and one of the currents goes through the coil $L_1$, the diode D1, the diode D5 and the capacitor $C_1$. Another current goes through the coil $L_2$, the diode D4, the diode D6 and the capacitor $C_2$. Simultaneously, the energy stored in the coils $L_1$ and $L_2$ is transferred to both capacitors. Thus there are two boost effects so called a "Double Boost Effect". The next equations come [3]:

$$Vs(t)-L_1\frac{d}{dt}i_{L1}(t)=V_{C1}(t) \quad (13)$$

$$i_{L1}(t)=i_{D1}(t)=i_{D5}(t) \quad (14)$$

$$L_2\frac{d}{dt}i_{L2}(t)=V_{C2}(t) \quad (15)$$

$$i_{L2}(t)=i_{D4}(t)=i_{D6}(t) \quad (16)$$

$$i_K(t)=i_{D2}(t)=i_{D3}(t)=0 \quad (17)$$

$$V_K(t)=-V_{D2}(t)=-V_{D3}(t)=V_{C1}(t)-L_2\frac{d}{dt}i_{L2}(t) \quad (18)$$

Now α depicts the PWM is duty cycle. Then the low frequency model of the power rectifier, when the mains voltage is positive i.e. where $\omega t\in]0;\pi[\mathrm{mod}[2\pi]$, is given by [3]:

$$\frac{V_{C1}(t)}{V_{S\max}\times\sin(\omega t)}=\frac{1}{1-\alpha}\times\frac{L_1}{L_1+L_2}+\frac{L_2}{L_1+L_2}-\frac{L_1\times i_{L1\max}\times\omega\times\cos(\omega t)}{V_{S\max}\times(1-\alpha)\times\sin(\omega t)} \quad (19)$$

$$\frac{V_{C2}(t)}{V_{S\max}\times\sin(\omega t)}=-\frac{\alpha}{1-\alpha}\times\frac{L_2}{L_1+L_2}+\frac{L_2\times i_{L2\max}\times\omega\times\cos(\omega t)}{V_{S\max}\times(1-\alpha)\times\sin(\omega t)} \quad (20)$$

Equation (19) shows that a Boost effect occurs on the capacitor $C_1$ and equation (20) shows that a Buck-Boost effect occurs on the capacitor $C_2$.

In short it can be noticed that assuming the coil $L_2$ value equals to zero, these equations can describe the single-phase VIENNA power cell too.

### 2.2 Negative mains voltage

When the switch K is closed (see Fig. 4 (a)), the diodes D2 and D3 are in the ON states and the current goes through the coil $L_1$, the diode D3, the switch K, the diode D2 and the coil $L_2$. Therefore the coils $L_1$ and $L_2$ store energy.

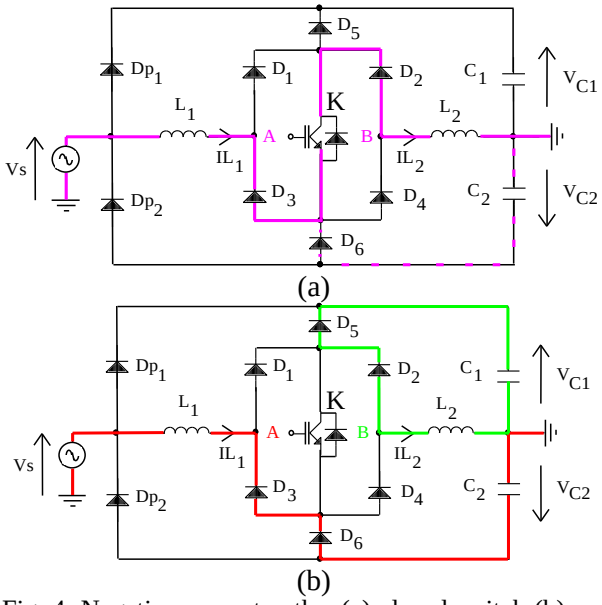


Fig. 4. Negative current paths: (a) closed switch (b) open switch [3]

During a very short time, a small part of the current $i_{L1}(t)$ goes to the diode D6 and the capacitor $C_2$. The next equations are obtained [3]:

$$Vs(t)-L_1\frac{d}{dt}i_{L1}(t)=L_2\frac{d}{dt}i_{L2}(t) \quad (21)$$

$$i_{L2}(t)=-i_K(t)=-i_{D2}(t) \quad (22)$$

$$i_{L1}(t)=-i_{D3}(t)=-i_{D6}(t)-i_K(t) \quad (23)$$

$$i_{D6}(t)>0 \quad (24)$$

$$-i_{L1}(t)>-i_{L2}(t) \quad (25)$$

$$i_{D6}(t)=i_{L2}(t)-i_{L1}(t) \quad (26)$$

$$V_{D6}(t)=0 \quad (27)$$

After a short time the diode D6 turns off and the currents $i_{L1}(t)$ and $i_{L2}(t)$ are equals [3]:

$$i_{D6}(t)=0 \quad (28)$$

$$V_{D6}(t)=V_{C2}(t)-Vs(t)+L_1\frac{d}{dt}i_{L1}(t) \quad (29)$$

Furthermore the following equations are always verified [3]:

$$i_{D1}(t)=i_{D4}(t)=i_{D5}(t)=0 \quad (30)$$

$$V_{D2}(t)=V_{D3}(t)=0 \quad (31)$$

$$V_{D5}(t)=Vs(t)-L_1\frac{d}{dt}i_{L1}(t)-V_{C1}(t) \quad (32)$$

When the switch K is open (see Fig. 4 (b)), the diodes D2, D3, D5 and D6 are in the ON states and one of the currents goes through the coil $L_1$, the diode D3, the diode D6 and the capacitor $C_2$. Another current goes through the coil $L_2$, the diode D2, the diode D5 and the capacitor $C_1$. Simultaneously, the energy stored in coil $L_1$ and coil $L_2$ is transferred to both capacitors. The next equations result [3]:

$$Vs(t)-L_1\frac{d}{dt}i_{L1}(t)=V_{C2}(t) \quad (33)$$

$$i_{L1}(t) = -i_{D3}(t) = -i_{D6}(t) \quad (34)$$

$$L_2 \frac{d}{dt} i_{L2}(t) = V_{C1}(t) \quad (35)$$

$$i_{L2}(t) = -i_{D2}(t) = -i_{D5}(t) \quad (36)$$

$$i_K(t) = i_{D1}(t) = i_{D4}(t) = 0 \quad (37)$$

$$V_K(t) = -V_{D1}(t) = -V_{D4}(t) = -Vs(t) + L_1 \frac{d}{dt} i_{L1}(t) + L_2 \frac{d}{dt} i_{L2}(t) \quad (38)$$

Using the duty cycle α and the previous equations, where $\omega t \in ]\pi;2\pi[\mathrm{mod}[2\pi]$, the low frequency model of the power rectifier, when the mains voltage is negative, is given by [3]:

$$\frac{V_{C2}(t)}{V_{S\max} \times \sin(\omega t)} = \frac{1}{1-\alpha} \times \frac{L_1}{L_1 + L_2} + \frac{L_2}{L_1 + L_2} - \frac{L_1 \times i_{L1\max} \times \omega \times \cos(\omega t)}{V_{S\max} \times (1-\alpha) \times \sin(\omega t)} \quad (39)$$

$$\frac{V_{C1}(t)}{V_{S\max} \times \sin(\omega t)} = -\frac{\alpha}{1-\alpha} \times \frac{L_2}{L_1 + L_2} + \frac{L_2 \times i_{L2\max} \times \omega \times \cos(\omega t)}{V_{S\max} \times (1-\alpha) \times \sin(\omega t)} \quad (40)$$

A "Double Boost Effect" occurs again. A Boost effect on the capacitor $C_2$ and a Buck-Boost effect on the capacitor $C_1$.

In short it can be noticed that assuming the coil $L_2$ value equals to zero, these equations can depict the single-phase VIENNA power cell too.

## 3. AC Current controller

### 3.1 Technics use in the AC current controller

In this paragraph an analog circuit controls the output current of a DC/AC converter and generates the PWM signal [13]. This analog circuit has been first involved in DC/AC converters with inductive loads and its method of controlling the power switches has been patented [14]. Its principle combines two ideas. This controller must act at lower frequencies for current regulation and it must act on higher frequencies for switching frequency control. In such way, an analog filter is added in the feedback loop in order to induce a phase-shift, which causes a self-oscillation. It is the reason why it is a PSSO current controller. So, the next figure (Fig. 5) shows one of its basic schemes:

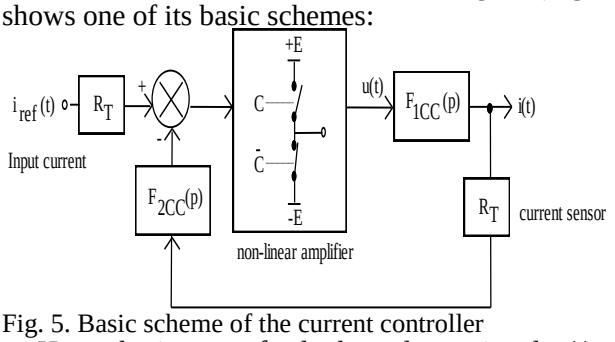


Fig. 5. Basic scheme of the current controller

Here, the inverter feeds the voltage signal $u(t)$ to an inductive load and the current sensor is used for feedback. The $F_{2CC}$'s filter is added in order to cause and control a self-oscillation. Thereafter, it controls the switching frequency of the power devices. Here it is located in the feedback loop. Nevertheless, it can be located between the error detector and the inverter [14], because it does not affect the low frequency signals. Then the transfer functions involved in this current controller are $F_{1CC}(p)$, $F_{2CC}(p)$ and $R_T$. They respectively depict the load voltage to current transfer function, the second order low-pass filter transfer function and the current sensor transfer one. They are given by:

$$F_{1CC}(p) = \frac{I(p)}{U(p)} = \frac{1}{r + Lp} = \frac{1}{r} . \frac{1}{1 + \tau_1 p} \quad (41)$$

$$F_{2CC}(p) = \frac{1}{1 + 2\xi_{CC} \frac{p}{\omega_{0CC}} + \frac{p^2}{\omega_{0CC}^2}} \quad (42)$$

Now, the transfer function $H_{CC}(p)$ relates to the linear part of the system. It takes into account the previous transfer functions $F_{1CC}(p)$, $R_T$ and $F_{2CC}(p)$, and then it is defined as follows:

$$H_{CC}(p) = F_{1CC}(p) * R_T * F_{2CC}(p)$$

$$H_{CC}(p) = \frac{R_T}{R} . \frac{1}{1 + \left(\tau_1 + \frac{2\xi}{\omega_{0CC}}\right) p + \left(\frac{2\xi\tau_1}{\omega_{0CC}} + \frac{1}{\omega_{0CC}^2}\right) p^2 + \frac{\tau_1}{\omega_{0CC}^2} p^3} \quad (43)$$

Thanks to this third order low-pass transfer function $H_{CC}(p)$, the system yields to a self-oscillation. The amplifier oscillates at the frequency where the feedback network has a 180 degrees phase-shift. The non-linear amplifier adjusts itself for unity loop gain at the switching frequency. This can be also written as the conditions of Heinrich Georg Barkhausen (1881-1956). So, taking into account a null reference, the phase-shift condition of Barkhausen permits to get the oscillation frequency $f_{osc}$ i.e. assuming the $H_{CC}(j\omega)$'s imaginary part equals zero. The gain's condition of Barkhausen permits to get the amplifier gain $A_0$ at the switching frequency i.e. assuming the $H_{CC}(j\omega)$'s real part equals unity. Then the oscillation frequency $f_{osc}$ and the amplifier gain $A_0$ are given by [13]:

$$\frac{f_{osc}}{f_{0CC}} = \frac{\omega_{osc}}{\omega_{0CC}} = \sqrt{1 + \frac{2\xi_{CC}}{\omega_{0CC}\tau_1}} = \sqrt{1 + 2\xi_{CC} . \frac{f_{c1}}{f_{0CC}}} \quad (44)$$

$$A_0 = 2\xi . \frac{r}{R_T} . (\omega_0 \tau_1 + \frac{1}{\omega_0 \tau_1} + 2\xi)$$

Now, for a better knowledge of the maximum switching frequency of the inverter, the load's time constant $\tau_1$ multiplied by the natural frequency $f_{0CC}$ of the $F_{2CC}$'s filter must be greater than 10. This is the case in the targeted applications. So, by comparing the $F_{1CC}$'s cut-off frequency $f_{c1}$ with the $F_{2CC}$'s natural frequency $f_{0CC}$, it can be observed that the oscillation frequency mainly depends on the $F_{2CC}$'s filter. It is slightly sensitive to the $F_{1CC}$'s parameters. Consequently the $F_{2CC}$'s filter controls the switching frequency of the power devices [14]. Its maximum value is given by the previous oscillation frequency [14].

### 3.2 Simulated and Experimental results

Now, experiments are done using both rectifiers, i.e. the DBE and the single-phase VIENNA one. In each case, the coil $L_1$ current is under control. Most of the parameter values are identical and they are given by $f = 50Hz$ (frequency), $V_{in} = 70Vrms$ (reduced mains voltage), $I_{refmax} = 6A$ (mains current reference), $C_1 = C_2 = 2200\mu F$ (DC bus capacitors), $R = 298\Omega$ (single load resistor). The experimental prototype involves a digital board, a power cell where an IRG4PH40PbF IGBT and STTH3012W power diodes are involved in. The AC current reference, synchronized with the network voltage, comes from a digital board which implements a 68HC11F1. An AD667 microprocessor-compatible 12-bit analog device digital-to-analog converter feeds the 6 Amps peak reference to the current controller. Current measurements are done thanks to sensors LEM LA25-NP. The DC output voltages are measured using the METRIX DIFFERENTIAL PROBE MX9003 and the DC voltage control is not implemented in the first time.

For the single-phase VIENNA rectifier power cell, there is a single coil $L_1$ whose value equals 3mH. Then two coils are involved in the DBE rectifier, where $L_1$ equals 820µH (AC side coil's inductance) and $L_2$ equals 2200µH. The sum of these two coil values is equal to the coil value involved in the single-phase VIENNA rectifier.

Thus, the next figures show the simulated and experimental results where the $L_1$ coil current is under control of the chosen PSSO current controller, where, the natural frequency of the second order low-pass filter is set to 18.4 kHz, and then the maximum switching frequency is limited to this value.

By viewing Fig. 7(a) and the third curve, i.e. without the $L_2$ coil, Fig. 6(b), the current ripples IL2 are very high, i.e. in the case of the single-phase VIENNA rectifier. It is not the case (see Fig. 9(a) and the third signal, Fig. 8(b)) when using the DBE rectifier. The ripple frequency of the voltages of both capacitors (capacitor $C_1$ and $C_2$ separately) is twice as high when using the DBE rectifier (see Fig. 9(b), Fig. 8(c)) in comparison with the single-phase VIENNA rectifier (see Fig. 7(b), Fig. 6(c) second and third curves).

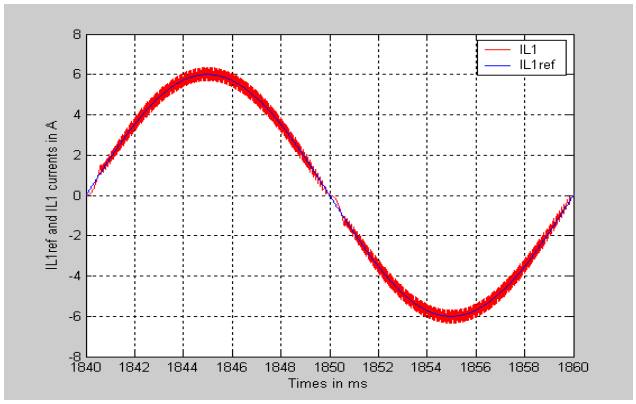


(a) $IL_{1ref}$ and $IL_1$currents

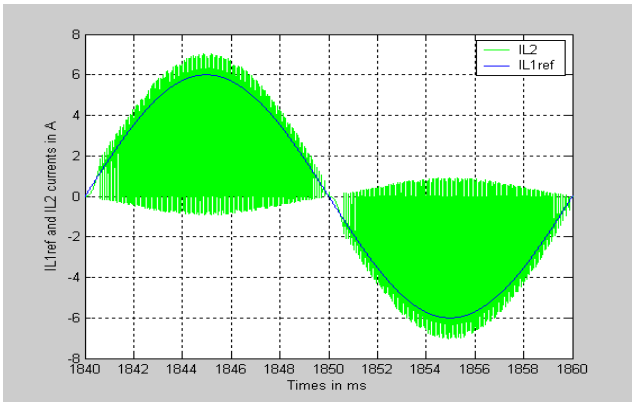


(b) $IL_{1ref}$ and $IL_2$ currents

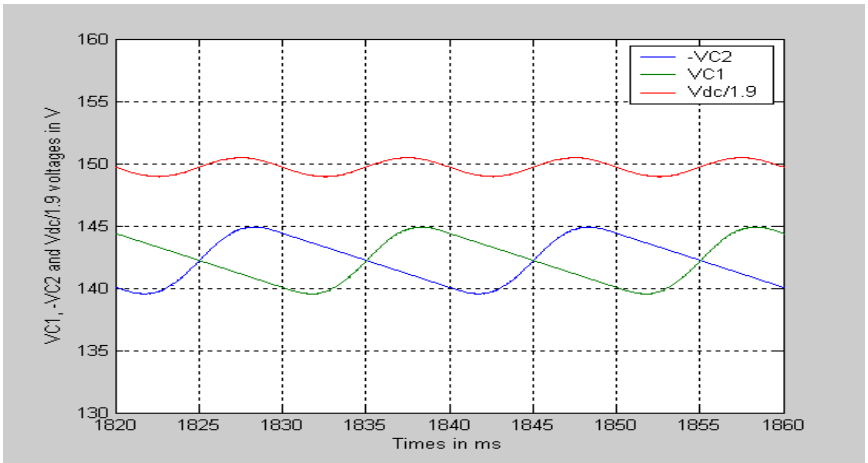


(c) $V_{C1}$, $V_{C2}$ and $V_{dc}$ voltages

Fig. 6. Simulated results: single-phase VIENNA rectifier

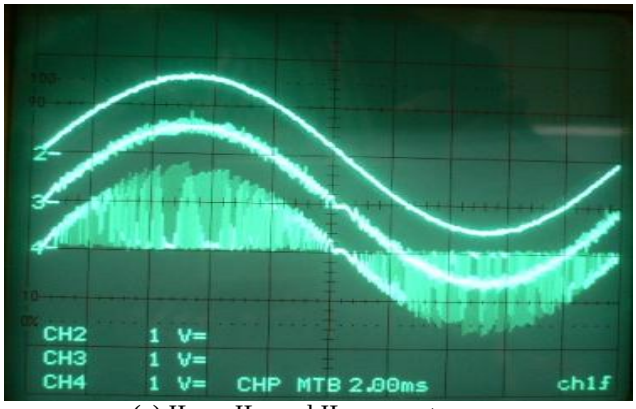


(a) $IL_{1ref}$, $IL_1$ and $IL_2$ currents

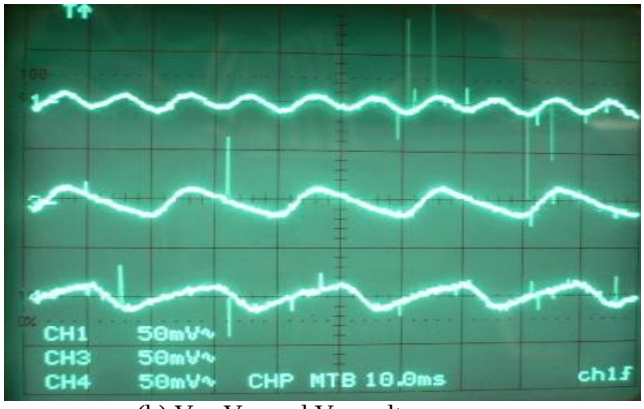


(b) $V_{dc}$, $V_{C1}$ and $V_{C2}$ voltages

Fig. 7: Experimental results using the single-phase VIENNA rectifier

In each spectrum a vertical division corresponds to 10dB and the bandwidth shown equals 12500Hz. The ripple amplitude (10V/div with a voltage sensor ratio of 1/200) of the voltages across both DC capacitors is lower when using the DBE (around 2Vpp see Fig. 9(b), Fig. 8(c)) in comparison with the single-phase VIENNA (around 5Vpp see Fig. 7(b), Fig. 6(c)). Thus, it could be possible to use lower values for the capacitors when using the DBE rectifier core.

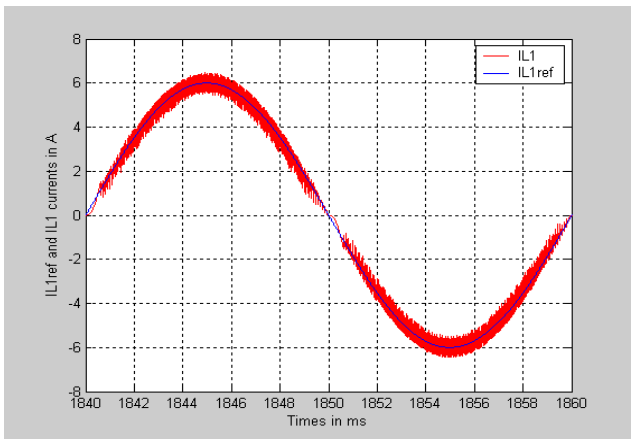


(a) $IL_{1ref}$ and $IL_1$ currents

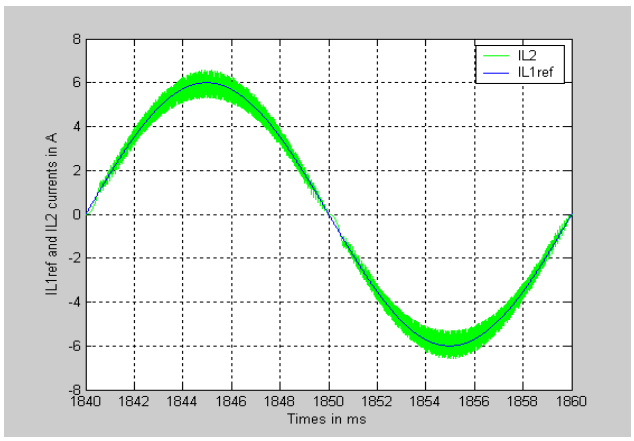


(b) $IL_{1ref}$ and $IL_2$ currents

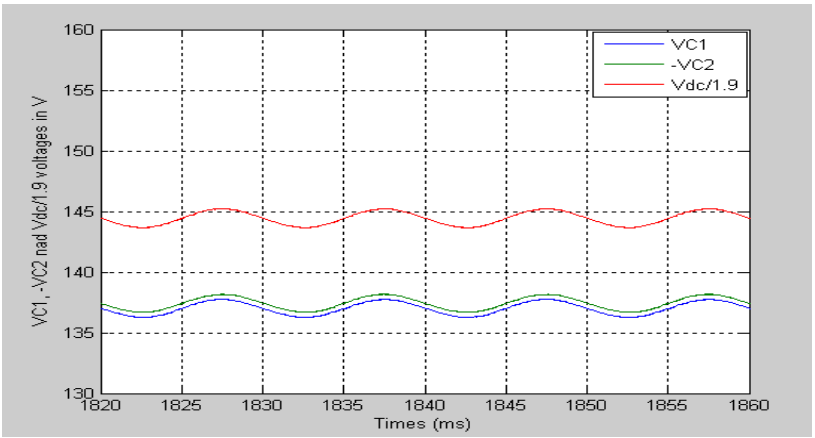


(c) $V_{C1}$, $V_{C2}$ and $V_{dc}$ voltages

Fig. 8. Simulated results: "DBE" rectifier, current control of the $L_1$ coil

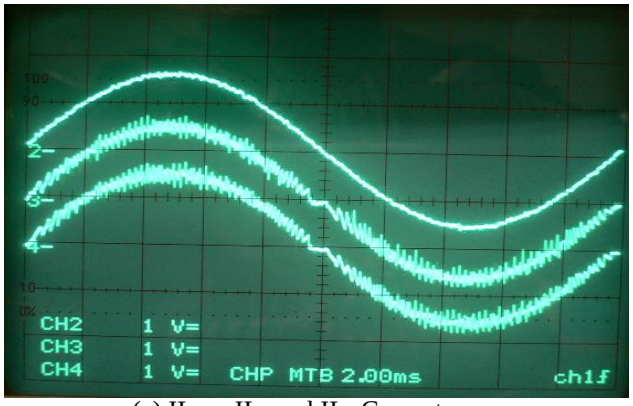


(a) $IL_{1ref}$, $IL_1$ and $IL_2$ Currents

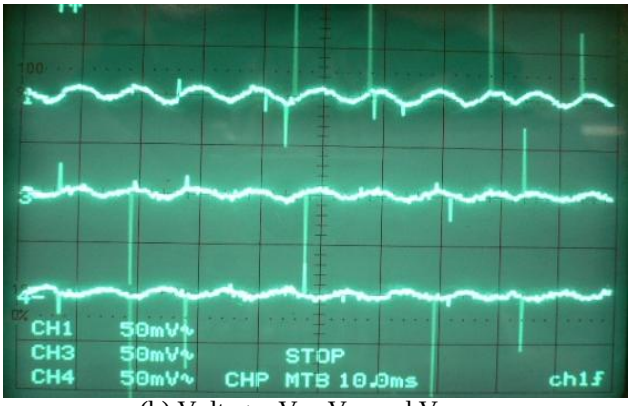


(b) Voltages $V_{dc}$, $V_{C1}$ and $V_{C2}$

Fig. 9. Experimental results using the DBE rectifier and the coil $L_1$ current control

From this analysis, to avoid the presence of high variation of current (di/dt) going through the ground connection, the DBE rectifier is preferred to the single-phase VIENNA. From the equations and the desired performances it is possible to optimize the values of the coil $L_1$ and the coil $L_2$. Furthermore, the results show that the IL1 current Total Harmonic Distortion of the DBE rectifier is lower when the control current is done on the coil $L_1$ in comparison with [2] where it was done on the coil $L_2$. This is normal because here it is the AC side coil current, which is under control.

## 4. DC Voltage controller

### 4.1 Technics used in the DC voltage controller

The determination of the parameters of the voltage controller requires the knowledge of the model of the rectifier i.e. the relation between the DC output voltage and the AC input current's amplitude drawn from the electrical network.

Now, assuming that the phase shift between the AC voltage and the AC current tends to zero (thanks to the current controller which accurately tracks its reference) and the rectifier losses can be neglected (i.e. the coil and the electronics devices losses are negligible), it comes:

$$V_{peak}.I_{peak}.(\sin(\omega t))^2 \approx C.V_{dc}\frac{dV_{dc}}{dt} + P_0 \quad (45)$$

$$V_{peak}.I_{peak}.\left(\frac{1-\cos(2\omega t)}{2}\right) \approx C.V_{dc}\frac{dV_{dc}}{dt} + P_0 \quad (46)$$

Where $P_0$ is only the instantaneous load power.

Then, the action of the voltage controller is to maintain the main value of the DC output voltage and to act at very low frequency. Then the equation becomes:

$$\frac{V_{peak}.I_{peak}}{2} \approx C.V_{dc}\frac{dV_{dc}}{dt} + P_0 \quad (47)$$

Thus, the next equations are obtained:

$$C.V_{dc}\frac{dV_{dc}}{dt} \approx \frac{V_{peak}.I_{peak}}{2} - P_0 \quad (48)$$

$$\frac{C}{V_{peak}}\frac{dV_{dc}^2}{dt} \approx I_{peak} - I_0 \quad (49)$$

Where $I_0 = \frac{2P_0}{V_{peak}}$ (50)

By introducing the Laplace variable 's' and considering the regulation of the square value of the DC voltage, it becomes:

$$V_{dc}^2(s) = \frac{V_{peak}}{Cs}\left(I_{peak} - I_0\right) \quad (51)$$

Assuming the current inner loop unitary (thanks to the current controller), the next figure shows the DC voltage control loop.

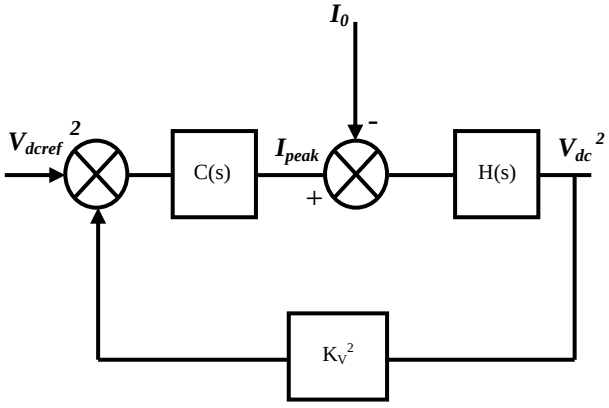


Fig. 10. DC voltage control loop

C(s) is a PI controller where $C(s) = K_p + \frac{K_i}{s}$ and $H(s) = \frac{V_{peak}}{Cs}$

The controller parameters are determined by using a classical synthesis method (pole placement method) and by considering $I_0$ as a disturbance. Thereby its parameters are given by:

$$K_p = \frac{2\xi C\omega_0}{K_v^2.V_{peak}} \quad (52)$$

$$K_i = \frac{C\omega_0^2}{K_v^2.V_{peak}} \quad (53)$$

Where $\xi = 0.707$ and $\omega_0.T_r = 3$; $T_r$ is the response time.

In order to ensure the Boost effect, the current amplitude to the voltage controller is flanged at a minimum and maximum value. The next figure (Fig. 11) shows the DC voltage controller scheme implemented in a Dspace system.

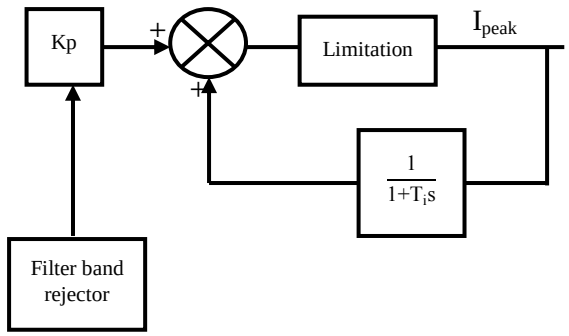


Fig. 11. DC voltage controller scheme

### 4.2 Experimental results

The DC voltage controller is implemented in a Dspace system. The parameters are given by f = 50Hz (frequency), $V_{in}$ = 70Vrms (reduced mains voltage), $V_{dcref}$ = 275V (DC reference voltage), Irefmax = 13A, Irefmin = 4.5A, C1 = C2 = 2200µF (DC bus capacitors), R1 = 298Ω, R2 = 333Ω. The load resistors R1 and R2 are in parallel. The resistor R2 is in series with a switch whose the switching frequency is equals to 0.6 Hz. Both resistors and the added switch represent the non-linear load. Fig. 12 gives an overview of the experimental bench.

Fig. 12. Experimental bench

The next figures show the experimental results and are obtained thanks to the Control desk software.

As shown in Fig. 13, for both tests performed on the "DBE" rectifier, the voltage succeeds in stabilize with a slight overshoot. When the load is non-linear (impact load about 50%), the variation voltage is about 6% in the transient (see Fig. 13(b)). The transient performances, for both tests, are excellent. By viewing Fig. 13(b), the ripple amplitude of the DC output voltage varies according to the load impact. Fig. 13(c) shows that the phase shift between the AC voltage and the AC current equals to zero and highlight the control strategy proposed. Fig. 13(d) shows the harmonic spectrums of DBE IL1 current and prove that the DBE rectifier respect the IEEE 519-1992 specification.

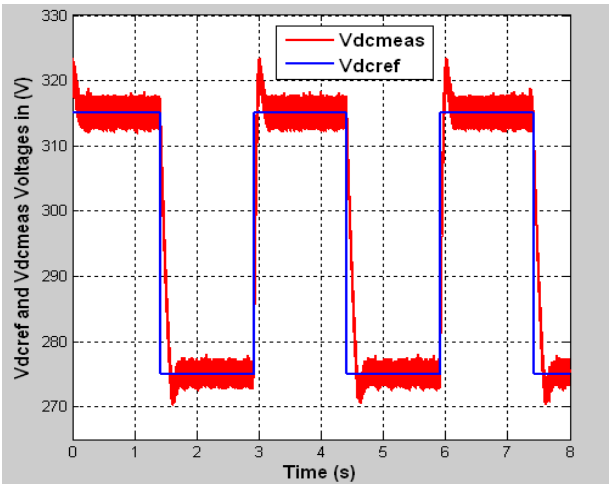


(a) Voltage steps

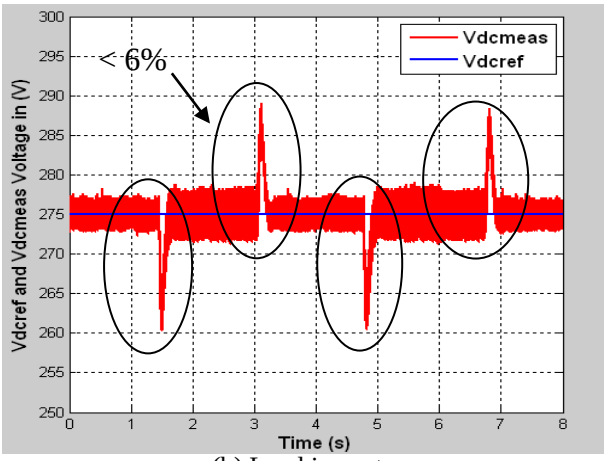


(b) Load impacts

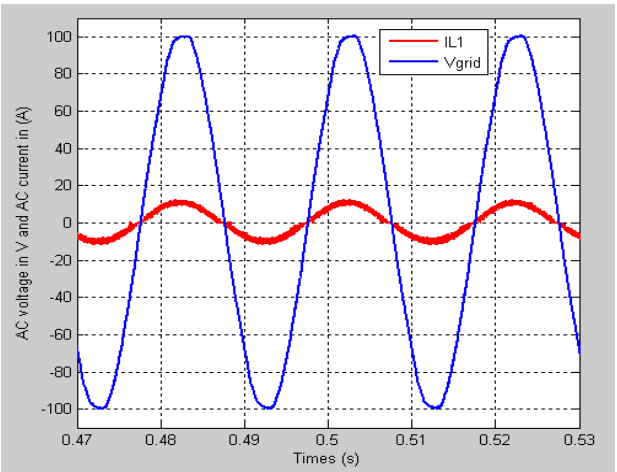


(c) $V_{grid}$ AC voltage and $IL_1$ AC current

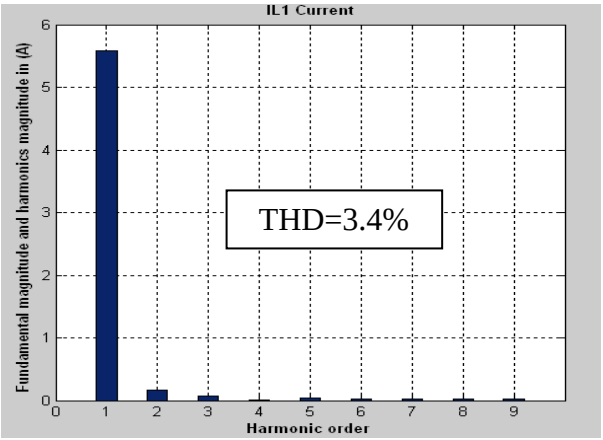

(d) IL1 Current Spectrum

Fig. 13. Experimental results "DBE" rectifier, DC voltage control

## 5. Conclusion

A new rectifier so called the DBE rectifier and its control has been investigated. In comparison with the single-phase VIENNA structure, the AC current ripple is lowered, and then the capacitor values can be reduced. Thanks to the inner control loop, which involves a Phase-Shifted Self-Oscillating Current-Controller (PSSO-CC), the external loop control becomes simple. Indeed, a simple PI can be used. Also, thanks to the current controller which accurately tracks its reference, the phase shift between the AC voltage and the AC current tends to zero. In conclusion, the proposed control strategy makes easier the control of such non-linear structure.

**References**

1. M. L. Heldwein, M. S. Ortmann, S. A. Amusa, "Single-phase PWM Boost-type Unidirectional Rectifier Doubling the Switching Frequency", 13th European Conference on Power Electronics and Applications, EPE 2009, Sept. 8-10, Barcelona, Spain, 2009.
2. J.C. Le Claire, G. Le Borgne, "Double Boost Effect Topology for AC/DC Converter with Unity Power Factor", PESC 2008, Rhodes, Greece, June 15-19, pp 3199-3205, CD-ROM ref. ISBN 978-1-4244-1668 4/08/$25.00.
3. J.C. Le Claire, "Double Boost Effect Topology for three-phase AC/DC Converter with Unity Power Factor", 13th European Conference on Power Electronics and Applications, EPE 2009, Sept. 8-10, Barcelona, Spain, 2009.
4. B. Singh, K. Al Haddad, A. Pandey, D. P. Kothari, "A Review of Single-Phase Improved Power Quality AC/DC Converters", IEEE Transactions on Industrial Electronics, Vol.50, N°5, pp 962-981, October 2003.
5. A. Pandey, D. P. Kothari, B. Singh, "Comparative Evaluation of Single-phase Unity Power Factor AC/DC Boost Converter Topologies", IE (I) Journal, Vol. 85, Sept. 2004, pp.102-109.
6. J. Herminjard, C. Zimmermann, R. Monnier, "Three-Phase Unity Power Factor AC/DC converter (PFC) with Dual Isolated C/DC Converter for a Battery Charger", EPE 1999, Lausanne, pp. 1-10.
7. N. Bernard, B. Multon, H. B. Ahmed, "le redresseur MLI en absorption sinusoïdale de courant", Revue 3EI N°35, December 2003, pp. 56-65.
8. Le Claire J.C, Radouane A., Ginot N., Moreau R., "Simple Topology and Current Control for Fast AC/DC Converter with Unity Power Factor", 11th International Power Electronics and Motion Control Conference, Riga, Latvia, 2-4 September 2004, CD-ROM ref. ISBN 9984-32-010-3.
9. J. C. Salmon, "Circuit Topologies for Single-phase Voltage-Doubler Boost Rectifiers", IEEE Transactions on Power Electronics, Vol. 8, n°4, October 1993, pp. 521-529.
10. Verdelho P. and Marques G. D., "DC Voltage Control and Stability Analysis of PWM-Voltage-Type Reversible Rectifiers", IEEE Transactions on Industrial Electronics, Vol. 45, N°2, April 1998, pp. 263-273.
11. Wang Z. and Chang L., "Dc-bus voltage control of three-phase ac/dc converter using load predictive method", Energy Conversion Congress and Exposition, 2009. ECCE 2009. IEEE, San Jose, California, September 2009, pp. 968-972.
12. Xu G., Xu L., Morrow D.J. and Chen D., "Coordinated DC Voltage Control of Wind Turbine With Embedded Energy Storage System", IEEE Transactions on Energy Conversion, Vol. 27, N°4, December 2012. pp. 1036-1045.
13. Le Claire J.C, Siala S., Saillard J., Le Doeuff R., "A new Pulse Modulation for Voltage Supply Inverter's Current Control", 8th European Conference on Power Electronics and Applications, Lausanne, Switzerland, September 1999, CD-ROM ref. ISBN 90-75815-04-2.
14. J.C. Le Claire, S. Siala, J. Saillard, R. Le Doeuff, US patent n° 6.376.935 B1, April 23, 2002, "Method and device for controlling switches in a control system with variable structure, with controllable frequency.